KRONOS FUSION ENERGY

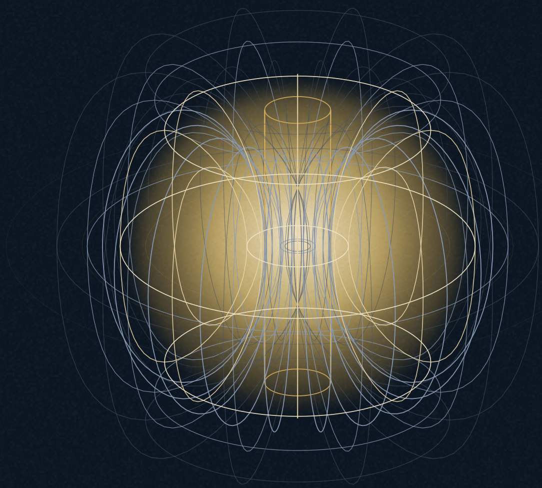

PAPER 2.32 · THE KRONOS 2026 SERIES

Breeding-Blanket and Neutron-Multiplier Concept Down-Select for a Compact Spherical-Tokamak Breeder: Ceramic versus Liquid-Metal Options Walking the TBR Ladder to Self-Sufficiency

For a breeder whose mission is tritium, helium-3 and 14 MeV neutrons—never net electricity—the blanket is the product line, and its design reduces to a concept down-select on one...

Read it live — 3-D model · physics validator · film series

BY P I FORD AND G L KULCINSKI

2026 · EDITORIAL EDITION

THE OFFICIAL RECORD

What this document is, and how to read its numbers

This is a combined editorial. It gathers, in one volume, the two design studies Kronos Fusion Energy released in 2026 — a compact spherical-tokamak tritium/helium-3 breeder and a deuterium–helium-3 tandem-mirror generator — together with the intellectual-property estate, the people, and, in the internal edition, the full commercial case. The scientific text is the same text that appears in the arXiv preprints and the journal submissions; the editorial adds the apparatus a reader needs to hold the whole program at once, and nothing in the physics is altered to fit it.

THE HONESTY STANCE IS THE ASSET

Every headline quantity carries an **evidence class** — DERIVED RECOMPUTED MEASURED REQUIREMENT — and, where a number is a modelled extrapolation rather than a demonstrated value, it is labelled as such and its downside is shown next to it. Several quantities in the underlying corpus moved after first publication; where a value has been withdrawn or restated, the record says so plainly. This is deliberate: a diligence team will find the load-bearing assumptions, so the document surfaces them first.

TWO EDITIONS

This volume is issued in two editions. The **public edition** (light) carries the physics and the design only — no dollar, price, or per-kilogram figure appears anywhere in it. The **internal edition** (dark) adds the economics, the funding architecture, and the defense-commercial analysis, and is marked *Confidential* accordingly; it is not for public distribution. Where the commercial case rests on a modelled assumption rather than a demonstrated one, it is labelled as such and its downside is shown alongside it, on the same terms as the physics.

TITLE	The Kronos Fleet — Hyperion · Aegis · MetroVolt: A Combined Design & Commercialization Study
AUTHOR	Priyanca Ford, Founder & CEO, on behalf of Kronos Fusion Energy
EDITION	2026 Combined Editorial · first issue
COMPANION WORKS	The five-paper arXiv drop — (1) Breeder, (2) Burner, (3) REBCO magnet & tape, (4) Direct Energy Conversion, (5) AI/ML/Quantum control — with matching numbered Zenodo deposits, plus the IOP journal and IAEA-FEC submissions. Patents were filed before the drop.
NAMING	Hyperion = the breeder; Aegis (defense) and MetroVolt (data-center) = one generator in two housings. Internal mode letters (D1, L) do not appear on public surfaces.
STATUS	Conceptual design & simulation study. Nothing herein is a construction commitment.

HOW TO READ THIS VOLUME

The fleet at a glance, and the way its numbers are marked

This volume opens with *Orientation*, presents the five research papers as a bound sequence, and closes with the *Apparatus*. *Foundations* sets out the three general results both machines rest on. *Paper One* is the Hyperion breeder; *Paper Two* the Aegis / MetroVolt generator; *Papers Three, Four and Five* are the enabling science — high-field REBCO magnets and tape, direct energy conversion, and the AI / ML / quantum control stack. A *Digital Twin & 3-D Model* part follows, then the *Environmental* profile. The *Economics* and levelized cost and the *Business Case* and diligence record appear in the internal edition only; the *Simulations* proof record and the Apparatus — patent portfolio, team, limitations, and sources — close both editions.

THE FLEET AT A GLANCE

	HYPERION	AEGIS	METROVOLT
Role	Strategic-isotope foundry	Defense installation power	Campus power
Machine	**Spherical tokamak**	**Tandem mirror**	**Tandem mirror**
Fuel	Deuterium–tritium	Deuterium–helium-3	Deuterium–helium-3
Delivers	Tritium · ^{3}He · 14 MeV n	Resilient installation power	Firm campus power
Physics bar	**Fusion gain only**	Closure (gates named)	Closure + lunar ^{3}He
In the fleet	Breeds the fuel	Proves the generator	Commercial destination

HOW THE NUMBERS ARE MARKED

Every headline quantity carries an evidence class — DERIVED from first principles, RECOMPUTED from raw data, MEASURED in hardware, or a REQUIREMENT yet to be met. Financial figures carry a case label and are confined to the internal (confidential) edition. Values that moved after first publication are shown as withdrawn or restated rather than quietly changed. A capability you can evaluate is one whose limits are on the page.

ABSTRACT

Breeding-Blanket and Neutron-Multiplier Concept Down-Select for a Compact Spherical-Tokamak Breeder: Ceramic versus Liquid-Metal Options Walking the TBR Ladder to Self-Sufficiency

For a breeder whose mission is tritium, helium-3 and 14 MeV neutrons—never net electricity—the blanket is the product line, and its design reduces to a concept down-select on one axis: the net tritium breeding ratio (TBR). We state the coupled neutron-transport, fuel-cycle, conjugate-heat-transfer and permeation problems formally, then rank the candidate blanket and neutron-multiplier concepts for the Hyperion breeder (design point $Q = 3.076$, $P_{\text{fus}} = 85.04\,MW$, $I_p = 9.66\,MA$, $\delta = -0.30$, $B_0 = 8\,T$, $\kappa = 2.0$, $R_0 = 1.20\,m$, aspect ratio $A = 2.5$, centrepost peak field 16.84 T) on a common three-dimensional continuous-energy Monte-Carlo footing (OpenMC/ENDF-B-VIII.0, 1.2×10^8 histories) and against the self-sufficiency bar $\Lambda \geq 1.05$. A bare recipe with no dedicated multiplier breeds only 0.742 and depletes a 2 kg inventory in 1.49 fpy; a beryllium-packed ceramic breeder (Be 9.6–11.8 vol %) reaches net TBR **1.026–1.062** (inboard mantle 0.2299 + outboard blanket 0.7960, leakage 0.12064), and a dedicated 5 cm solid-beryllium multiplier layer lifts the same lever to **1.18–1.20**; outboard-blanket thickness alone moves it to 1.24–1.25 at 65–$80\,cm$. Self-sufficiency is *resolved* in the as-drawn three-dimensional CAD geometry at net TBR 1.12 (single null) and 1.07 (double null). On the breeder-form axis, a self-cooled liquid-lithium blanket passes thermally with a reduced-activation ferritic-martensitic (RAFM) structure at 516 °C ($+34$ margin) where an as-configured helium-cooled ceramic (HCPB) bed runs to 712 °C, and liquid lithium retains tritium roughly 6.7 orders of magnitude better than tin. The selection is a beryllium-multiplied ceramic blanket as the baseline breeder with a self-cooled-lithium blanket as the thermally robust alternative; the multiplier thickness is the one lever that trades against the centrepost shield in the radial budget.

Open-access deposit (code & data, CC BY 4.0): DOI 10.5281/zenodo.22645937 · Zenodo community *kronos_fusion_energy*. Explore it live: interactive 3-D model · physics validator.

Keywords: tritium breeding ratio, beryllium multiplier, ceramic breeder, liquid lithium, blanket down-select, neutronics, conjugate heat transfer

CONTENTS

Table of Contents

NOMENCLATURE

Symbols, units, and the names of things

Q	plasma (fusion) gain, P_{fus}/P_{aux}
Q_E	engineering gain, net electric out / recirculating in
H_{98}	confinement enhancement over the IPB98(y,2) scaling
Z_{eff}	effective ion charge
c_{ee}	electron–electron bremsstrahlung leading coefficient, 2.120022 (exact)
τ_E	energy confinement time
I_p	plasma current
R_0, a	major radius, minor radius
κ, δ	elongation, triangularity
β_N	normalized plasma beta (Troyon-normalized)
TBR	tritium breeding ratio
DEC	direct energy conversion
CF	plant capacity factor (availability)
FOAK / NOAK / BOAK	first / n^{th} / best of a kind
Hyperion	the ST breeder (internal: Mode D2)
Aegis	the generator, defense/installation housing (internal: Mode M)
MetroVolt	the generator, data-center housing (Mode M)

tritium breeding ratio; beryllium multiplier; ceramic breeder; liquid lithium; blanket down-select; neutronics; conjugate heat transfer

§ 1

Introduction

THE BREEDER AS A MATERIALS MACHINE

The Hyperion breeder is a materials machine, not a power plant. Its outputs are tritium for the fuel cycle, helium-3 banked from tritium decay, and a 14 MeV neutron source for isotope production and irradiation testing; its success criterion is breeding, never net electricity [1,2,3]. That reframing is not rhetorical. It moves the blanket from a piece of balance-of-plant into the central product, and it makes the entire engineering question a concept down-select on a single figure of merit—the net tritium breeding ratio Λ (tritons bred per fusion neutron, after leakage and the inboard shield). Every candidate blanket and every candidate neutron multiplier is admitted or rejected by where it sits on that one axis relative to the self-sufficiency bar, and every other property—thermal margin, tritium retention, activation, maturity—is a constraint that a passing concept must additionally clear.

WHY A COMPACT SPHERICAL TOKAMAK MAKES BREEDING HARD

A compact spherical tokamak (ST) confines a large plasma current in a small volume, which is what makes it an attractive neutron source and breeder platform [32,33], but it also makes the breeding problem harder than in a large aspect-ratio device. The inboard side is occupied by the centrepost carrying the toroidal field (16.84 T peak at the conductor) and by the tungsten-carbide shield that protects it; there is almost no room for an inboard breeding mantle. The consequence is geometric and unforgiving: most of the tritium must be bred in the outboard blanket, the solid angle available for breeding is reduced, and the neutron budget is tight. In our reference three-dimensional model the inboard mantle contributes only $\Lambda_{,\mathrm{in}} = 0.2299$ against the outboard $\Lambda_{,\mathrm{out}} = 0.7960$ (§4). Neutron *multiplication* is therefore not an optimization luxury; it is the enabling lever that carries a compact ST from sub-unity breeding to self-sufficiency.

PRIOR ART

The two mature solid-breeder lines are the helium-cooled pebble bed (HCPB), in which lithium-orthosilicate or metatitanate ceramic pebbles are interleaved with a beryllium or beryllide neutron multiplier [19,20,21], and the helium-cooled or water-cooled lithium-lead (HCLL/WCLL) lines, in which the Pb-15.7Li eutectic is both breeder and multiplier [22,21]. Liquid-metal concepts—self-cooled or dual-cooled lithium and lithium-lead—trade the pebble bed's manufacturing maturity for a flowing breeder that carries its own tritium out of the vessel and tolerates higher volumetric heating [23,24,25]. Neutron multiplication in fusion blankets has been understood since the earliest blanket studies [17,18]; the modern beryllide multipliers ($Be_{12}Ti$, $Be_{12}V$) were developed precisely to raise the multiplier operating temperature and suppress the helium-driven swelling that limits metallic beryllium [26,27,28]. The condition for tritium self-sufficiency—that the net TBR exceed unity by a margin sufficient to cover losses, radioactive decay, startup inventory and a doubling requirement—was placed on a rigorous footing by Abdou and co-workers [29,30,31], whose analysis frames the design target we adopt here.

CONTRIBUTION

This paper puts the candidate blanket and multiplier concepts side by side on one common, physically explicit footing and states the selection. Our specific contributions are: (i) a formal statement of the coupled neutron-transport, fuel-cycle, conjugate-heat-transfer and tritium-permeation problems that jointly define blanket viability (§2); (ii) a common three-dimensional continuous-energy Monte-Carlo evaluation of every concept on the frozen operating point, executed on the NVIDIA GPU HPC campaign (§3); (iii) a decomposition of the net TBR into an additive inboard/outboard ledger and into separable design levers—multiplication, thickness, coverage—so that the down-select is transparent rather than a single opaque number (§4); and (iv) the selection itself, a beryllium-multiplied ceramic baseline with a self-cooled-lithium alternative, together with the one radial-budget trade that governs it (§5–§7). Throughout we treat Λ as a design *lever* —a family of valid blanket points—rather than a single fixed number, because the compact ST's shield-dominated inboard makes coverage, not intrinsic breeding chemistry, the binding constraint. The result complements the companion Kronos studies that established the cross-library breeding-fleet case [4], the CAD-faithful three-dimensional neutronics that resolves the net TBR in real geometry [5], the dedicated beryllium and $Be_{12}Ti$ multiplier down-select [7], the per-unit tritium ladder and doubling time [8], the blanket and divertor thermal-hydraulics [11], and the liquid-lithium-over-tin wall-chemistry choice [12].

§ 2

Governing equations and the formal problem

The down-select is decided by four coupled physics problems. We state each as a boundary- or initial-value problem, identify the functional that maps a blanket design vector to its figure of merit, and then cast the selection itself as a constrained decision.

THE DESIGN VECTOR AND THE SELECTION PROBLEM

Let a blanket concept be described by a design vector

$$d = \big(m,\ f_{\mathrm{Be}},\ t_{\mathrm{b}},\ e_6,\ f_{\mathrm{cov}},\ \phi_{\mathrm{form}}\big),$$

with multiplier type $m \in \{\varnothing, \textbf{packed Be}, \textbf{solid Be}, \textbf{Be}_{12}\textbf{Ti}\}$, beryllium volume fraction f_{Be}, outboard breeding-zone radial thickness t_{b}, lithium-6 enrichment e_6, effective three-dimensional breeding coverage f_{cov}, and breeder form $\phi_{\mathrm{form}} \in \{\textbf{ceramic}, \textbf{liquid Li}, \textbf{PbLi}\}$. Three scalar responses are computed from d at the frozen operating point: the net breeding ratio $\Lambda(d)$, the peak structure temperature $T_{\max}(d)$, and the tritium retention/permeation margin $\Pi(d)$. The down-select is the constrained feasibility-then-ranking problem

$$\begin{array}{lll} \text{find} & d \in \mathcal{D} & \text{such that} \\ \text{(S1)} & \Lambda(d) \ge \Lambda^\star = 1.05, & \\ \text{(S2)} & T_{\max}(d) \le T_{\lim} = 550\,^\circ\mathrm{C}, & \\ \text{(S3)} & \text{waste class}(d) \preceq \text{Class C}, & \\ \text{(S4)} & t_{\mathrm{b}}(d) + t_{\mathrm{sh}} \le R_{\mathrm{budget}} & \text{(radial-space closure)}, \end{array}$$

ranked by technological maturity and fuel-cycle robustness among the feasible set. Equations (2)–(2) are the machine-checkable contract that the rest of this section makes concrete.

TRITIUM FUEL-CYCLE BALANCE AND THE SELF-SUFFICIENCY CONDITION

The mobile in-vessel tritium inventory $I(t)$ obeys the fuel-cycle balance

$$\frac{\mathrm{d}I}{\mathrm{d}t} = \dot N_{\mathrm{bred}} - \dot N_{\mathrm{burn}} - \lambda_{\mathrm{T}} I - \dot L_{\mathrm{loss}}, \qquad \dot N_{\mathrm{bred}} = \Lambda\,\dot N_{\mathrm{burn}},$$

where $\dot N_{\mathrm{burn}} = \dot m_{\mathrm{burn}}$ is the tritium burn rate, $\lambda_{\mathrm{T}} = \ln 2/\tau_{1/2}$ is the tritium decay constant ($\tau_{1/2} = 12.32\,yr$), and $\dot L_{\mathrm{loss}}$ collects permeation, trapping and processing losses. The burn rate follows directly from the fusion power. With $E_{\mathrm{DT}} = 17.6\,MeV$ per D–T reaction, each reaction consuming one triton,

$$\dot m_{\mathrm{burn}} = \frac{P_{\mathrm{fus}}}{E_{\mathrm{DT}}}\,m_{\mathrm{T}} = \frac{85.04\,\mathrm{MW}}{17.6\,\mathrm{MeV}}\,(3.016\,\mathrm{u}) \ \approx\ 3.02\times10^{19}\ \mathrm{s}^{-1} \ \approx\ 4.769\,\mathrm{kg/fpy},$$

which is the register anchor (BR-L1-A6). Writing the losses as an effective fraction folded into the net ratio, the quasi-steady tritium surplus available as product is the affine law

$$S(\Lambda) \ =\ \dot m_{\mathrm{burn}}\,(\Lambda - 1) \ -\ \lambda_{\mathrm{T}} I_{\mathrm{ss}},$$

whose slope is exactly $\dot m_{\mathrm{burn}}$. Neglecting the small decay term against the anchor calibration, $S = \dot m_{\mathrm{burn}}(\Lambda - 1)$ reproduces the register outputs to the reported precision: $S = 1.6215\,kg/fpy$ at $\Lambda = 1.34$ and $S = 3.8152\,kg/fpy$ at $\Lambda = 1.80$ (BR-OUT-1), a per-unit export of 1 kg/fpy at $\Lambda = 1.2097$ and 2 kg/fpy at $\Lambda = 1.4194$ (BR-L2-A11h). The self-sufficiency condition (S1) is the requirement that (3) admit a non-decreasing inventory once startup, decay and a doubling allowance are covered,

$$\Lambda \ \ge\ \Lambda^\star \ =\ 1 + \varepsilon_{\mathrm{loss}} + \frac{\lambda_{\mathrm{T}} I_{\mathrm{ss}}}{\dot m_{\mathrm{burn}}} + \varepsilon_{\mathrm{doubling}} \ \approx\ 1.05,$$

and the startup inventory required before breeding begins is $I_{\mathrm{start}} = \dot m_{\mathrm{burn}}\,\tau_{\mathrm{start}}$, i.e.\ $2.38/4.77/9.54\,kg$ for $\tau_{\mathrm{start}} = 0.5/1/2\,yr$ (BR-L1-A6). Equation (3) also makes the failure mode quantitative: at the coverage-honest $\Lambda = 0.742$ the source term is negative, $S \simeq -1.28\,kg/fpy$, and a 2 kg inventory falls to 0.64 kg at one year and depletes at 1.49 fpy. Sub-unity breeding is therefore not a small deficit to be trimmed; it is a hard no-go, and multiplication is the only lever that closes it.

THE NEUTRON-TRANSPORT PROBLEM AND THE TBR FUNCTIONAL

The angular neutron flux $\psi(\mathbf{r}, \hat{\Omega}, E)$ in the blanket obeys the steady linear Boltzmann transport equation

$$\hat{\Omega}\cdot\nabla\psi + \Sigma_t(\mathbf{r}, E)\,\psi = \int_{4\pi} \mathrm{d}\hat{\Omega}' \int_0^\infty \mathrm{d}E'\,\Sigma_s(\mathbf{r}, E' \to E, \hat{\Omega}' \to \hat{\Omega})\,\psi(\mathbf{r}, \hat{\Omega}', E') + \frac{S_n(\mathbf{r}, E)}{4\pi},$$

with Σ_t, Σ_s the macroscopic total and double-differential scattering cross sections and S_n the fusion neutron source. The source is not free: its spatial shape is the plasma neutron emissivity, set by the free-boundary MHD equilibrium poloidal flux $\psi_{eq}(R, Z)$ through the fusion reactivity $S_n(\mathbf{r}) \propto \frac{1}{4} n_D n_T \langle\sigma v\rangle_{DT}(T_i(\mathbf{r}))$, emitting a $14.06\,MeV$ spectrum. The scalar flux is $\phi(\mathbf{r}, E) = \int_{4\pi} \psi\,\mathrm{d}\hat{\Omega}$. The gross tritium breeding ratio is the reaction-rate functional

$$\Lambda_{gross} = \frac{1}{N_{src}} \int_V \mathrm{d}\mathbf{r} \int_0^\infty \mathrm{d}E \left[N_6\,\sigma^{Li6}_{(n,t)}(E) + N_7\,\sigma^{Li7}_{(n,n'\alpha)t}(E) \right] \phi(\mathbf{r}, E),$$

summing the exothermic ${}^6\mathrm{Li}(n, \alpha)\mathrm{t}$ channel (dominant at thermal and epithermal energies) and the endothermic ${}^7\mathrm{Li}(n, n'\alpha)\mathrm{t}$ channel (a fast-spectrum contributor above $\sim 2.5\,MeV$). The *net* ratio subtracts what the geometry loses,

$$\Lambda = \Lambda_{gross} - L_{leak} - P_{par}, \qquad L_{leak} = \frac{1}{N_{src}} \oint_{\partial V} \mathbf{J}\cdot\hat{\mathbf{n}}\,\mathrm{d}A,$$

with L_{leak} the boundary leakage and P_{par} the parasitic capture on structure, coolant and shield. Neutron multiplication enters as a source-doubling reaction that raises the population available to (8): per source neutron the available population is $1 + M$, with

$$M = \frac{1}{N_{src}} \int_V \mathrm{d}\mathbf{r} \int \mathrm{d}E \left[N_{Be}\,\sigma^{Be}_{(n,2n)}(E) + 2\,N_{Be}\,\sigma^{Be}_{(n,3n)}(E) + \ldots \right] \phi.$$

Because $\sigma_{(n,2n)}$ for ${}^9\mathrm{Be}$ has a threshold near $1.85\,MeV$ and rises through the $14\,MeV$ source region, multiplication is most effective on the un-degraded fast flux at the front of the blanket—which is why a dedicated multiplier layer placed *ahead* of the breeder outperforms the same beryllium distributed through a moderated bed. Finally, the shield-dominated inboard makes the net ratio naturally additive over the poloidal solid angle,

$$\Lambda = \Lambda_{,in} + \Lambda_{,out},$$

the decomposition we report and exploit in §4.

LEVERS AND THE COVERAGE DISCOUNT

Equations (8)–(10) expose Λ as a smooth functional of $\mathbf{d}$ with three separable, monotone levers. The *multiplication* lever raises the population feeding (8); at fixed geometry $\partial\Lambda/\partial f_{Be} > 0$ until self-shielding of the beryllium saturates M. The *thickness* lever raises the optical depth of the breeding zone; for an exponentially attenuating fast flux the incremental capture saturates as

$$\Lambda(t_b) \;\simeq\; \Lambda_\infty - \left(\Lambda_\infty - \Lambda_0\right) e^{-t_b/\ell},$$

with ℓ an effective attenuation length, so $\partial\Lambda/\partial t_b > 0$ but diminishing. The *coverage* lever is multiplicative and is the compact ST's binding term: the reduced-order chemistry is discounted by the fraction of the neutron-emitting solid angle actually subtended by breeding material,

$$\Lambda^{3D} \;\approx\; f_{cov}\,\Lambda^{1D}, \qquad 0 < f_{cov} \le 1.$$

A literal one-dimensional recipe that breeds above unity can fall below it once the inboard shield, ports and divertor cut-outs are resolved; conversely a modest chemistry margin plus high coverage clears the bar. This is why the three-dimensional evaluation (§3) is not a refinement of the ladder but its arbiter.

BREEDER-FORM VIABILITY: CONJUGATE HEAT TRANSFER

A concept that breeds must also be coolable. In the solid structure and breeder the temperature field obeys the steady conduction equation with the volumetric nuclear heating $q_n'''(\quad r)$ taken directly from the neutronics deposition tally,

$$\nabla\cdot\big(k(T)\,\nabla T\big) + q_n'''(\quad r) = 0,$$

coupled at the wetted surfaces to the coolant energy equation $\rho c_p(\partial_t T + \quad u\cdot\nabla T) = \nabla\cdot(k\nabla T) + \Phi$ closed by a turbulent wall-heat-transfer coefficient $h = \mathrm{Nu}\, k_f/D_h$ with $\mathrm{Nu} = \mathrm{Nu}(\mathrm{Re}, \mathrm{Pr})$. The coolant mass flow required to remove blanket power Q_{blk} at allowable temperature rise ΔT is $\dot{m} = Q_{\mathrm{blk}}/(c_p\Delta T)$; for the helium loop ($c_p = 5193\,J/kgK$, $\Delta T = 200\,K$, $Q_{\mathrm{blk}} = 95\,MW$) this is $\dot{m} = 91.7\,kg/s$ (BV-06). The viability constraint (S2) is that the peak structure temperature stay under the RAFM limit,

$$T_{\max} = \max_{r\in\mathrm{struct}} T(\quad r) \;\le\; T_{\mathrm{lim}} = 550\,^{\circ}\mathrm{C}.$$

For the helium-cooled ceramic (HCPB) bed this couples back to geometry: (15) is met only if the first-wall channel is held to $\le 6\,mm$ depth and $\le 15\,mm$ pitch (BR-SX-15); a self-cooled liquid-lithium blanket carries the heat in the flowing breeder itself and meets (15) with margin.

TRITIUM TRANSPORT IN THE BREEDER: DIFFUSION–TRAPPING AND PERMEATION

The fuel-cycle loss term $\dot{L}_{\mathrm{loss}}$ in (3) and the retention margin $\Pi(\quad d)$ are set by tritium transport through the breeder and structure. We model the mobile concentration C_{m} and trapped concentration C_{t} by the McNabb–Foster diffusion–trapping system

$$\frac{\partial C_{\mathrm{m}}}{\partial t} = \nabla\cdot\big(D(T)\nabla C_{\mathrm{m}}\big) - \frac{\partial C_{\mathrm{t}}}{\partial t} + S_{\mathrm{g}},$$
$$\frac{\partial C_{\mathrm{t}}}{\partial t} = k_{\mathrm{tr}}(T)\,C_{\mathrm{m}}\,(n_{\mathrm{t}} - C_{\mathrm{t}}) - p_{\mathrm{dt}}(T)\,C_{\mathrm{t}},$$

with $D(T) = D_0 e^{-E_D/k_B T}$ the diffusivity, $k_{\mathrm{tr}}, p_{\mathrm{dt}}$ the Arrhenius trapping/de-trapping rates, n_{t} the trap density and S_{g} the generation rate. At a wetted surface the boundary condition is the Sieverts law $C_{\mathrm{m}} = K_S(T)\sqrt{p_{\mathrm{T_2}}}$, and a permeation-barrier coating of permeation-reduction factor (PRF) reduces the through-wall steady flux by the same factor, $J_{\mathrm{perm}} = \Phi_{\mathrm{perm}}\sqrt{p_{\mathrm{T_2}}}/(\mathrm{PRF}\cdot L)$. The retention margin Π that differentiates breeder forms is dominated by the breeder's tritium solubility: pure lithium retains tritium roughly 6.7 orders of magnitude more strongly than tin and 4.6 orders more strongly than Pb-15.7Li, giving a $\sim 7000\,hour$ breakthrough buffer (BR-SX-03), while candidate barrier coatings ladder as Al_2O_3 (PRF $\sim 10^3$) $>$ Er_2O_3 ($\sim 3\times10^2$) $>$ TiC $>$ TiN. Equations (16)–(16) therefore close the mission-critical accountancy: the breeder that retains tritium best protects the very inventory that (3) tracks.

§ 3

Computational methodology: the NVIDIA GPU HPC campaign

Every quantitative claim in this paper is produced by the Kronos NVIDIA GPU HPC campaign; the reduced-order and analytic fuel-cycle layers run alongside on an in-house HPC node so that the transport fleet is never idle. This section names the codes actually run for this paper, the acceleration and problem scale, and the verification that makes the numbers reproducible. No cost figures are reported anywhere; the campaign is described by its physics and its scale only.

THREE-DIMENSIONAL MONTE-CARLO NEUTRON TRANSPORT

The transport equation (7) and the functionals (8)–(10) are solved by the continuous-energy Monte-Carlo code OpenMC [13,14] with ENDF/B-VIII.0 nuclear data [15]. The as-drawn blanket, first-wall, multiplier, shield and centrepost geometry is carried into the transport solver by the DAGMC CAD-to-Monte-Carlo pipeline [16], so that (13) is evaluated on the real three-dimensional coverage rather than an idealized cylinder; the companion CAD-faithful neutronics paper [5] documents the STEP-to-DAGMC path in full. The fusion source S_{n} samples the equilibrium emissivity of the frozen operating point ($Q = 3.076$, $P_{\mathrm{fus}} = 85.04\,MW$, $\delta = -0.30$). Each reference balance uses $N = 1.2 \times 10^8$ source histories; tritium production, $(n, 2n)$ multiplication, boundary leakage, first-wall fast flux and cell-wise nuclear heating are scored as track-length and surface-current tallies. The statistical error on the reference net TBR is $\pm 0.010\%$ (one standard deviation). Weight-window variance reduction, generated from an adjoint importance map, concentrates histories in the deep-penetration inboard shield where the breeding contribution $\Lambda_{,\mathrm{in}}$ is otherwise poorly resolved.

GPU acceleration and scale. The Monte-Carlo campaign runs event-based particle transport across the NVIDIA GPU HPC fleet (A100/H100/A10 partitions), which is what makes the lever sweeps tractable: the TBR ladder is not a single run but a family of transport solves over f_{Be}, t_{b}, multiplier type and coverage, each converged to sub-per-mille statistics, plus a Pb-15.7Li cross-library arbiter run [4]. The event-based GPU pathway keeps the many-configuration sweep within a single campaign, so that the ladder of Table 2 and figure 2 is internally consistent (identical source, geometry and data across every point).

DEPLETION, ACTIVATION AND WASTE CLASSIFICATION

The activation constraint (S3) is evaluated by coupling the transport solution to a Chebyshev-rational (CRAM-48) depletion solve of the Bateman equations on the real first-wall spectrum, giving the two-full-power-year activation inventory and the ALARA waste class of every component (BR-L1-A10). The result—all components Class C or better with no greater-than-Class-C waste, only tritium pushing past Class A—is reported by the companion activation and waste-routing study [6] and enters here only as the feasibility gate (2).

CONJUGATE HEAT TRANSFER AND DISCRETIZATION

The breeder-form thermal problem (14)–(15) is solved by a two-dimensional conjugate heat-transfer (CHT) model that takes the volumetric heating q'''_{n} directly from the neutronics deposition tally, so that the thermal and neutronic solutions share a single source of truth (BR-SX-15). The conduction operator is discretized by a second-order finite-volume scheme on a boundary-refined mesh; the coupled solid–fluid interface uses a conjugate flux-continuity condition $k_s \partial_n T|_s = k_f \partial_n T|_f$ with the turbulent wall coefficient $h(\mathrm{Re}, \mathrm{Pr})$. Convergence is declared when the peak-temperature residual falls below 10^{-4} of T_{lim} and the global energy imbalance closes to better than 0.5%; the reported peak temperatures ($516\,^{\circ}C$ self-cooled Li, $712\,^{\circ}C$ as-configured HCPB) are mesh-converged to within a few degrees. The three heat-removal loops—blanket 95 MW helium, first wall 5 MW, divertor 12 MW water, total pumping 5.8 MW (5.2%)—are closed by a one-dimensional network model (BV-06) whose per-loop mass flows follow from $\dot{m} = Q/(c_p \Delta T)$.

VERIFICATION, REPRODUCIBILITY AND PROBLEM SCALE

Three verification gates are enforced. First, a neutron-balance closure: the reference run reports leakage 0.12064 ± 0.00003, net TBR $1.0258 \pm 0.010\%$ decomposed as inboard 0.2299 + outboard 0.7960, $(n, 2n)/\mathrm{source} = 0.0339$, first-wall fast flux ($E > 0.1\,MeV$) $6.999 \times 10^{14}\,\mathrm{n\,cm^{-2}s^{-1}}$, and nuclear heating 74.6 MW of the 85.04 MW fusion power, which balance to the source term (BR-L1-A5). Second, a fuel-cycle anchor match: the surplus law (5) reproduces its register anchors exactly at $\Lambda = 1.34$ and 1.80 (BR-OUT-1). Third, a cross-library arbiter: an independent Pb-15.7Li transport model agrees with the lithium-metal net TBR to within $+0.004$ (register head-to-head), confirming the ranking is not a single-library artifact. All decks—the OpenMC/DAGMC transport inputs, the CRAM-48 depletion deck, the CHT model and the fuel-cycle scripts—are archived with the deposit and regenerate every number in this paper.

§ 4

Results

THE REFERENCE NEUTRON ECONOMY

Table 1 collects the reference three-dimensional balance for the beryllium-packed ceramic recipe, and figure 1 displays it. The net TBR of 1.0258 is not a monolith: it is the additive ledger of equation (11), an inboard mantle contributing 0.2299 and an outboard blanket contributing 0.7960. The compact ST's geometry is visible directly in that split—the outboard carries 78% of the breeding because the inboard is shield-dominated. Multiplication contributes a modest $(n, 2n)/\text{source} = 0.0339$ in the dilute-packing reference, leakage removes 0.12064, and $74.6\,MW$ of the $85.04\,MW$ fusion power deposits as recoverable nuclear heating. These five numbers close the neutron balance to the source term at 1.2×10^8 histories.

QUANTITY	VALUE	NOTE
net TBR Λ (n,Xt on Li)	$1.0258 \pm 0.010\%$	inboard 0.2299 + outboard 0.7960
boundary leakage L_{leak}	0.12064 ± 0.00003	escaping source neutrons
$(n, 2n)$ multiplication M	$0.0339 \pm 0.4\%$	dilute Be in reference recipe
first-wall fast flux ($E > 0.1\,MeV$)	6.999×10^{14}	$\text{n}\,\text{cm}^{-2}\text{s}^{-1}$, outboard W FW
nuclear heating	74.6 MW	of 85.04 MW fusion
tritium burn rate $\dot{m}_{\text{burn}}$	$4.769\,\text{kg/fpy}$	eq. (4)

Reference three-dimensional neutron economy for the beryllium-packed ceramic recipe (BR-L1-A5), OpenMC/ENDF-B-VIII.0, 1.2×10^8 histories. Per-source-neutron quantities unless noted.

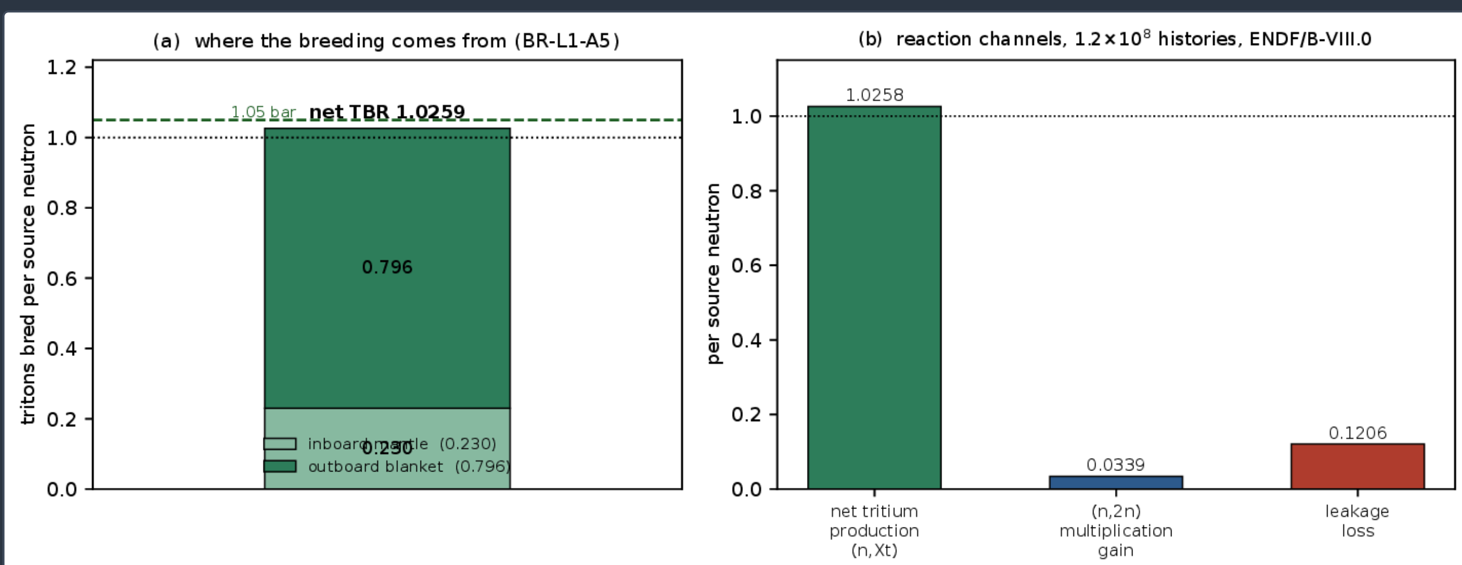

Reference neutron economy (BR-L1-A5). (a) The net TBR of 1.0258 as the additive inboard-mantle (0.2299) plus outboard-blanket (0.7960) ledger of equation (11), against the $\Lambda \geq 1.05$ self-sufficiency bar. (b) The real reaction channels that set the ratio—net tritium production, $(n, 2n)$ multiplication gain, and boundary-leakage loss—each a tally per source neutron at 1.2×10^8 histories on ENDF/B-VIII.0.

THE TBR LADDER BY CONCEPT

Table 2 and figure 2(a) rank the candidate concepts on this common footing. A bare recipe with no dedicated multiplier breeds only **0.742**—below unity, and quantified by (3) as a hard no-go. Packing beryllium into the ceramic bed at **9.6–11.8** vol % supplies $(n, 2n)$ multiplication in place and lifts the net ratio across the self-sufficiency bar: **1.026** at **0.65** packing fraction and **1.062** at **0.80** (BR-L1-A5, BR-L2-A7). Replacing distributed packing with a dedicated 5 cm solid-beryllium layer ahead of the breeder—where equation (10) is most effective on the un-degraded fast flux—lifts the same lever to **1.18–1.20** (BR-L2-A7), the register's upper endpoint, reached without changing anything else. Beryllide multipliers ($Be_{12}Ti$) are the higher-temperature, lower-swelling variant of this layer, down-selected on the same footing in the companion multiplier study [7,26,27]: they trade a small multiplication penalty for markedly better helium retention and swelling behaviour.

BLANKET / MULTIPLIER CONCEPT	NET TBR	NOTE	SERIAL
bare recipe, no dedicated multiplier	0.742	sub-unity, non-starter	ladder floor
ceramic + Be packing (0.65 fill)	1.026	3-D MC reference	BR-L1-A5
ceramic + Be packing (0.80 fill)	1.062	same lever, higher fill	BR-L2-A7
ceramic + 5 cm solid-Be layer	1.18–1.20	dedicated multiplier layer	BR-L2-A7
outboard blanket 65/80 cm	1.241/1.254	thickness lever	BR-L2-A11h
advanced multi-lever stack	1.419	→ 1.99 *kg*-T/unit/yr	BR-L2-A7u
self-cooled liquid Li (form axis)	breeds + $^{7}Li(n, n'\alpha)$	PASS 516 °C	BR-SX-15
He / HCPB ceramic (as configured)	—	over-limit 712 °C	BR-SX-15

Blanket and neutron-multiplier concepts for the Hyperion breeder, scored on the common three-dimensional Monte-Carlo footing. "Net TBR" is after leakage and the inboard shield. Serials are Physics De-Risking Register entries.

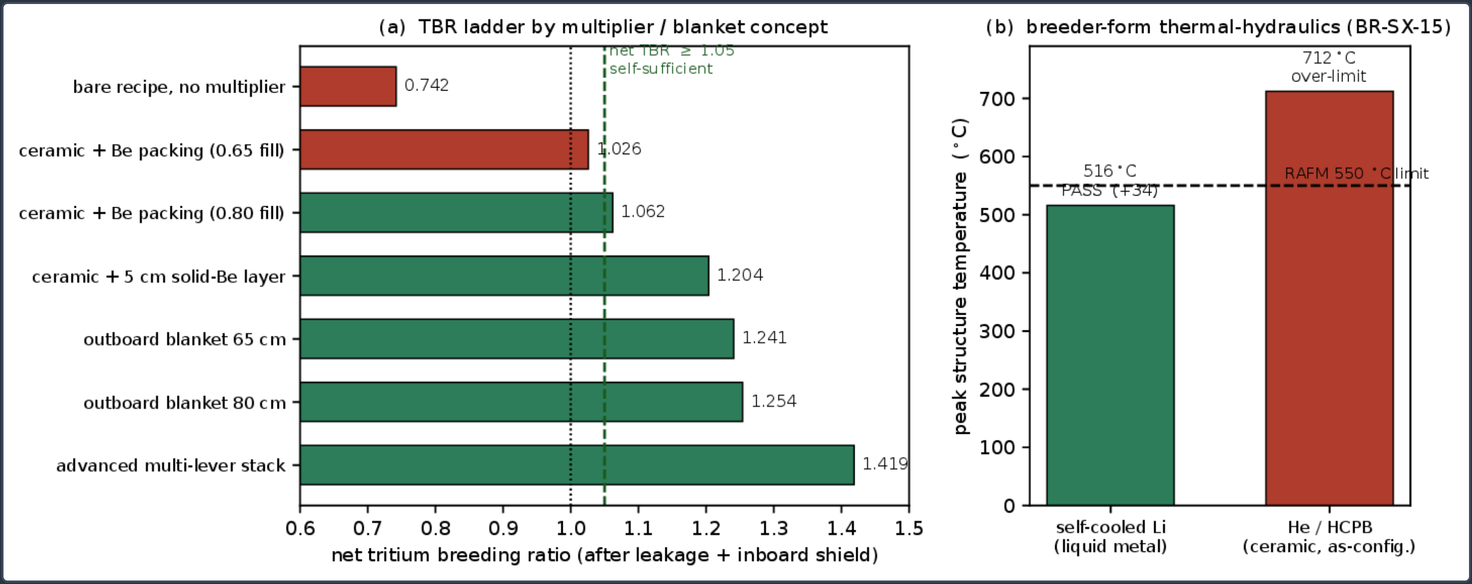

The blanket and neutron-multiplier down-select. (a) TBR ladder by concept: a bare recipe breeds **0.742** (below the $\geq$ **1.05** bar), beryllium packing reaches **1.03**–**1.06**, a dedicated 5 cm beryllium layer **1.20**, and blanket thickness **1.24**–**1.25**; green bars clear the self-sufficiency bar and red bars do not. (b) Breeder-form thermal-hydraulics (BR-SX-15): a self-cooled liquid-lithium blanket passes at 516 °C where an as-configured helium-cooled ceramic bed runs over-limit at 712 °C against the 550 °C RAFM limit.

THE SURPLUS LAW AND THE COST OF SUB-UNITY BREEDING

Figure 3 plots the fuel-cycle consequences. Panel (a) is the affine surplus law (5): its slope is $\dot{m}_{\mathrm{burn}} = 4.769\,kg/fpy$, it passes exactly through the register anchors (BR-OUT-1), and it locates the export set-points—$\Lambda = 1.2097$ for 1 kg/fpy, 1.4194 for 2 kg/fpy. Panel (b) integrates the inventory ODE (3) for two contrasting cases: at the coverage-honest $\Lambda = 0.742$ the inventory falls from 2 kg to 0.64 kg at one year and depletes at 1.49 fpy, whereas at the three-dimensional CAD single-null point $\Lambda = 1.12$ the inventory grows. The figure makes the central physical statement visible: multiplication is what moves the design from the red trajectory to the green one, and it is not optional in a compact ST.

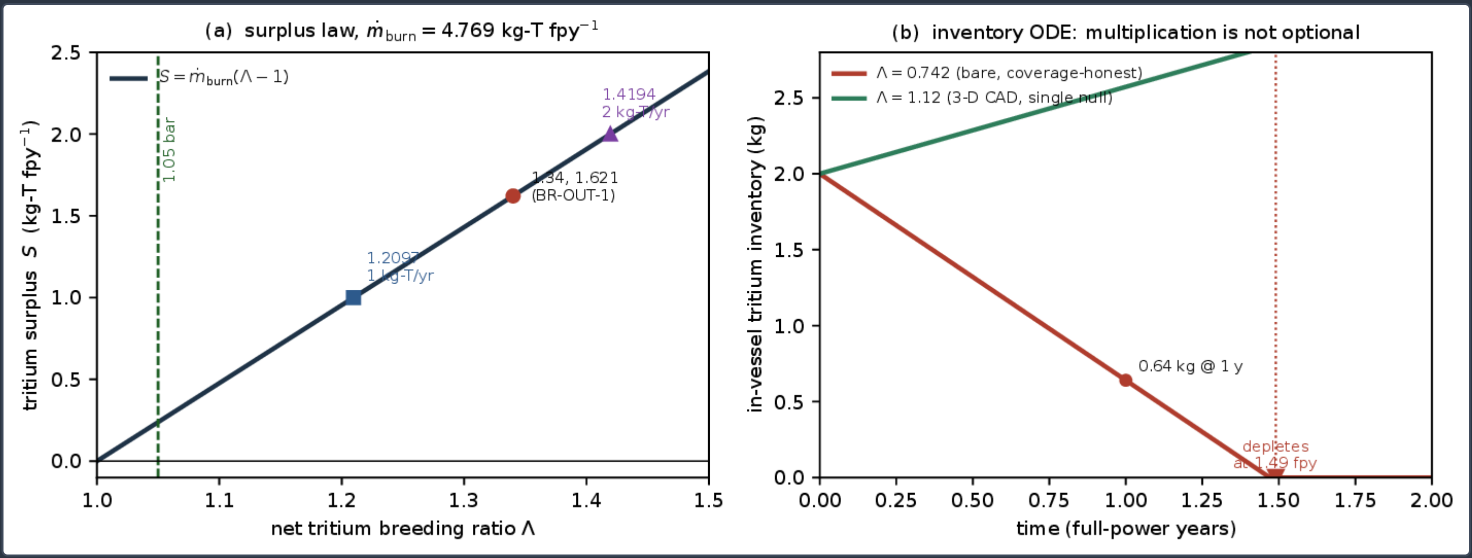

Fuel-cycle consequences of the breeding lever. (a) The affine surplus law $S = \dot{m}_{\mathrm{burn}}(\Lambda - 1)$ of equation (5), slope $\dot{m}_{\mathrm{burn}} = 4.769\,kg/fpy$, through the BR-OUT-1 anchor at $\Lambda = 1.34$ and the 1- and 2 kg/fpy export set-points. (b) Integration of the inventory ODE (3): sub-unity $\Lambda = 0.742$ depletes a 2 kg inventory at 1.49 fpy; the resolved 3-D CAD single-null point $\Lambda = 1.12$ grows it.

THE THICKNESS LEVER AND THE THREE-DIMENSIONAL RESOLUTION

Independently of the multiplier, deepening the outboard blanket raises the net ratio monotonically with the saturating behaviour of equation (12): **1.2407** at 65 cm and **1.2545** at 80 cm, with a multi-lever stack reaching **1.4194** at the 2 kg/fpy export point (BR-L2-A11h, BR-L2-A7u). Figure 4 plots this lever together with the arbiter that matters most: the self-sufficiency claim is confirmed where it is hardest to confirm, on the as-drawn three-dimensional CAD geometry, at net TBR **1.12** for a single-null configuration and **1.07** for the double null that the divertor down-select favours [9]—both above the ≥ 1.05 bar. Tritium self-sufficiency is therefore not a reduced-model claim but a resolved three-dimensional result. Thickness is the cleanest lever, but figure 4 also shows why it is not free: past $\sim 80\,cm$ it competes with the centrepost shield for radial space, the one open trade of §6.

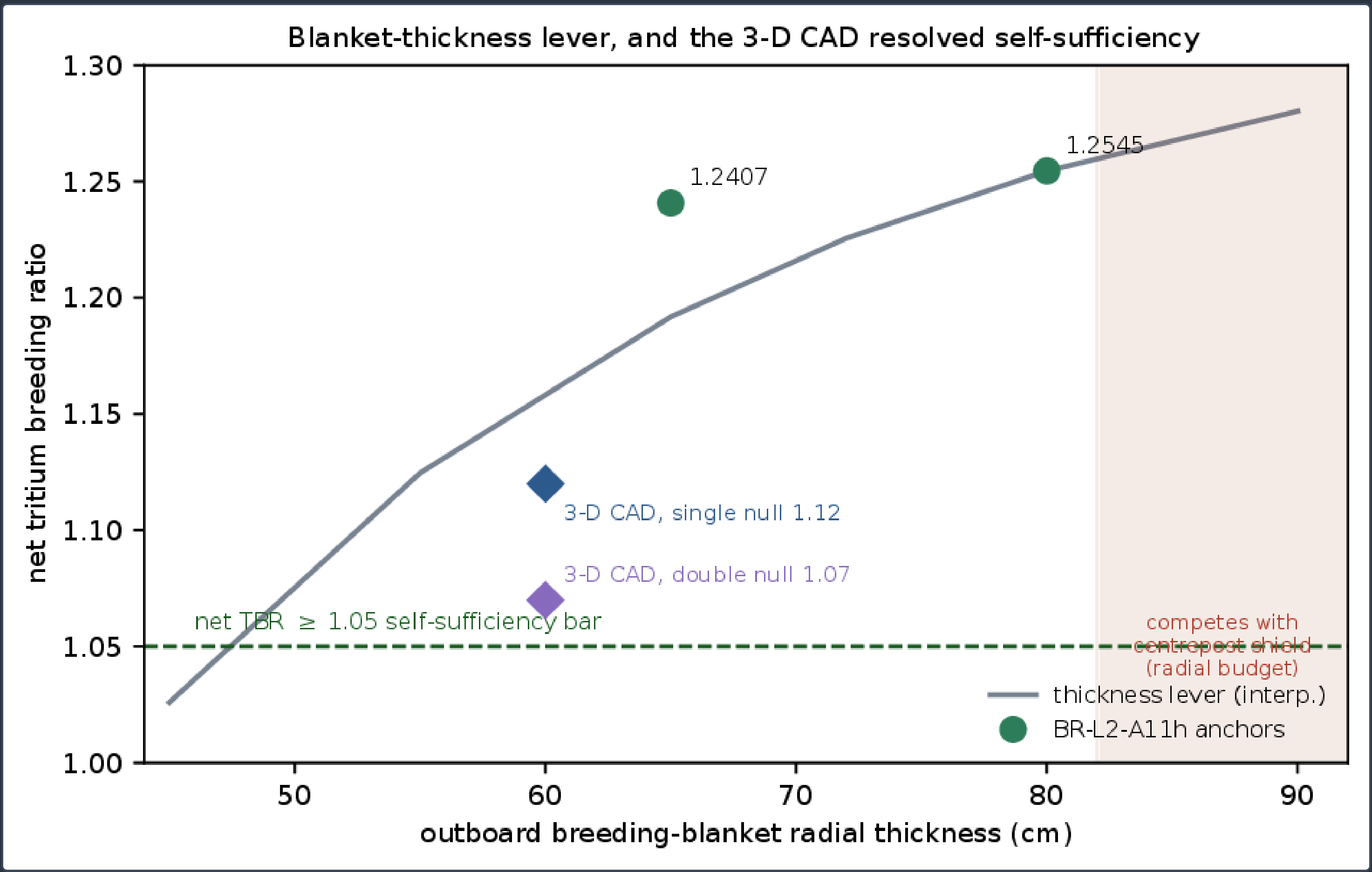

Blanket-thickness lever and the three-dimensional resolution. The saturating lever of equation (12) through the BR-L2-A11h anchors (65 cm $\rightarrow$ 1.2407, 80 cm $\rightarrow$ 1.2545), with the resolved 3-D CAD self-sufficiency points 1.12 (single null) and 1.07 (double null) marked as diamonds. Beyond $\sim 80\,cm$ (shaded) the lever competes with the centrepost shield in the radial budget (2).

THE COVERAGE DISCOUNT

Figure 5 shows why the three-dimensional evaluation is the arbiter rather than the reduced-order ladder. The coverage discount of equation (13) multiplies every one-dimensional lever by $f_{cov} < 1$, and because the ST inboard is shield-dominated the discount is real. The literal beryllium-packed recipe (one-dimensional 1.026) falls below breakeven once coverage is applied; the solid-beryllium lever (one-dimensional ~ 1.20) clears the bar only above $f_{cov} \approx 0.87$–0.91, and the coverage-hardening study (HX-02) reports 91% coverage on that lever as the self-sufficiency requirement. The advanced multi-lever stack (one-dimensional 1.42) carries margin even under a substantial coverage discount. The resolved 3-D CAD points ($1.12/1.07$) already have the coverage folded in and sit above the bar, which is the sense in which self-sufficiency is de-risked rather than assumed.

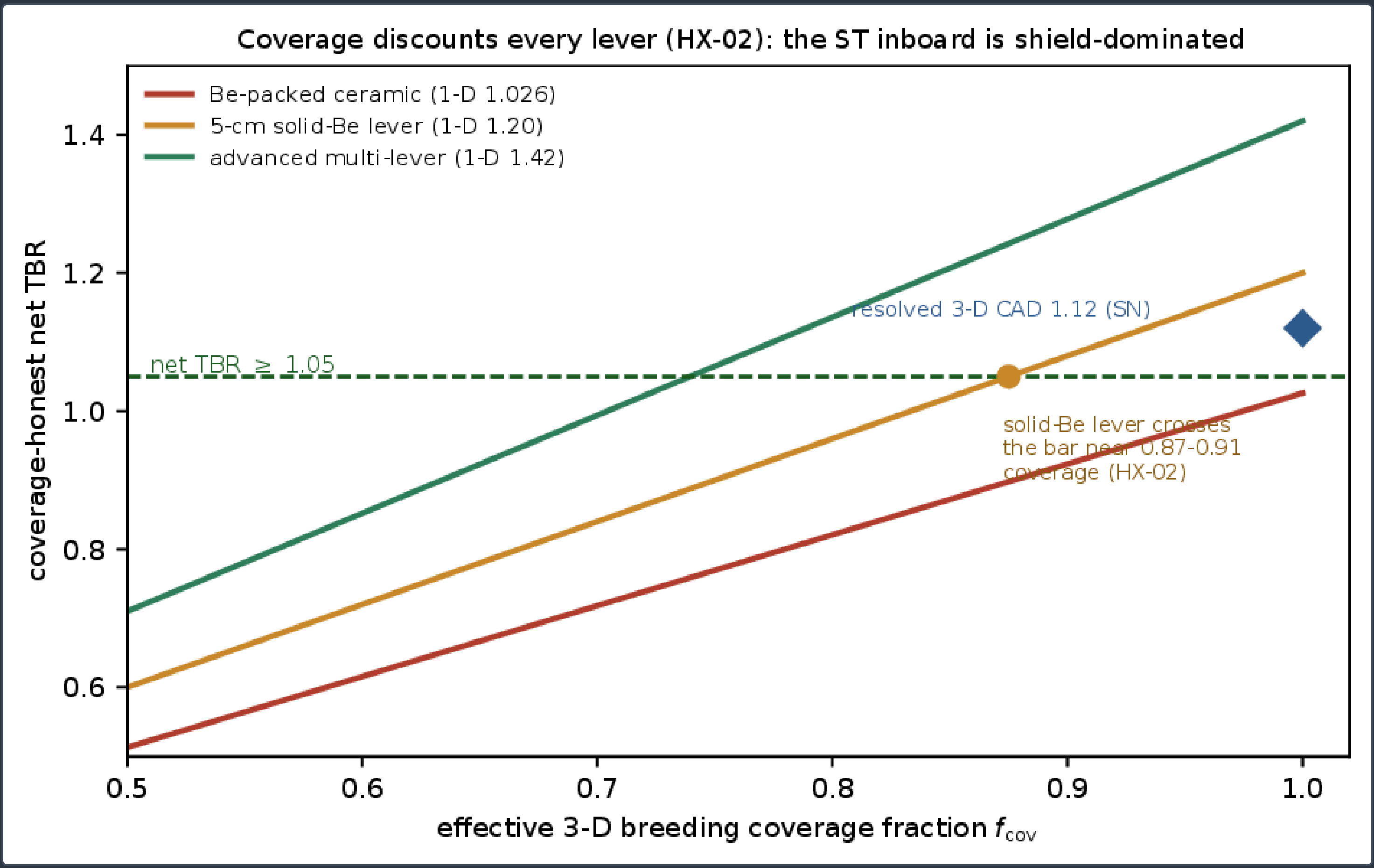

The coverage discount (HX-02, equation 13). Each one-dimensional lever is multiplied by the effective three-dimensional coverage fraction f_{cov}; the ST's shield-dominated inboard makes the discount binding. The reference recipe crosses below the bar; the solid-Be lever needs $f_{cov} \approx 0.87$ -0.91; the advanced stack keeps margin. The resolved 3-D CAD single-null point (1.12) already folds coverage in.

BREEDER FORM: THERMAL-HYDRAULICS AND THE LOOP BUDGET

On the form axis the decision is thermal robustness, not breeding. Figure 2(b) and figure 6 report the conjugate-heat-transfer verdict (BR-SX-15) and the loop budget (BV-06). A self-cooled liquid-lithium blanket both breeds and multiplies via ${}^7\mathrm{Li}(n, n'\alpha)$ and passes thermally: the RAFM structure sits at 516 °C, a 34 °C margin under its limit, because the flowing breeder carries its own heat. An as-configured helium-cooled ceramic (HCPB) bed runs over-limit to 712 °C and meets equation (15) only if the first-wall channel is held to $\leq 6\,mm$ depth and $\leq 15\,mm$ pitch. The three-loop heat-removal budget closes at 5.2% pumping power (blanket 95 MW helium at $\dot{m} = 91.7\,kg/s$, first wall 5 MW, divertor 12 MW water); the divertor peak flux of $8\,MW/m^2$ against the CuCrZr coolable cap of $4\,MW/m^2$ is what makes detachment mandatory, addressed in the divertor portfolio [9].

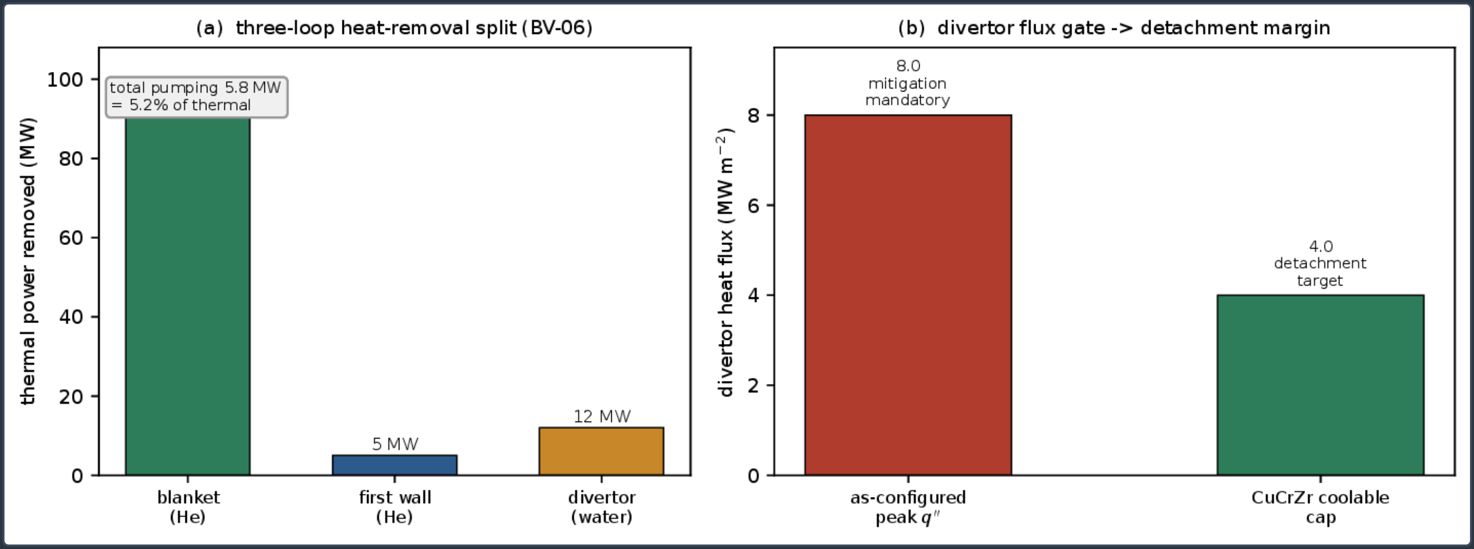

Heat-removal budget (BV-06). (a) Three-loop split—blanket 95 MW helium, first wall 5 MW helium, divertor 12 MW water—with total pumping $5.8\,\mathrm{MW}$ (5.2% of thermal). (b) The divertor as-configured peak heat flux ($8\,MW/m^2$) against the CuCrZr coolable-flux cap ($4\,MW/m^2$), setting the detachment requirement.

BREEDER FORM: THE TRITIUM BARRIER

Liquid lithium also wins decisively on the fuel cycle. Figure 7 plots the retention and barrier ladders of BR-SX-03: pure lithium retains tritium roughly $\mathbf{6.7}$ orders of magnitude more strongly than tin and $\mathbf{4.6}$ orders more strongly than Pb-15.7Li, with a $\sim 7000\,hour$ break-through buffer, and the candidate barrier coatings ladder as Al_2O_3 ($\mathbf{PRF} \sim 10^3$) $>$ Er_2O_3 ($\sim 3 \times 10^2$) $>$ TiC $>$ TiN. Through equations (16)–(16) this is the property that protects the very inventory the mission depends on; the wall-chemistry choice is developed in full in the companion permeation-barrier study [12].

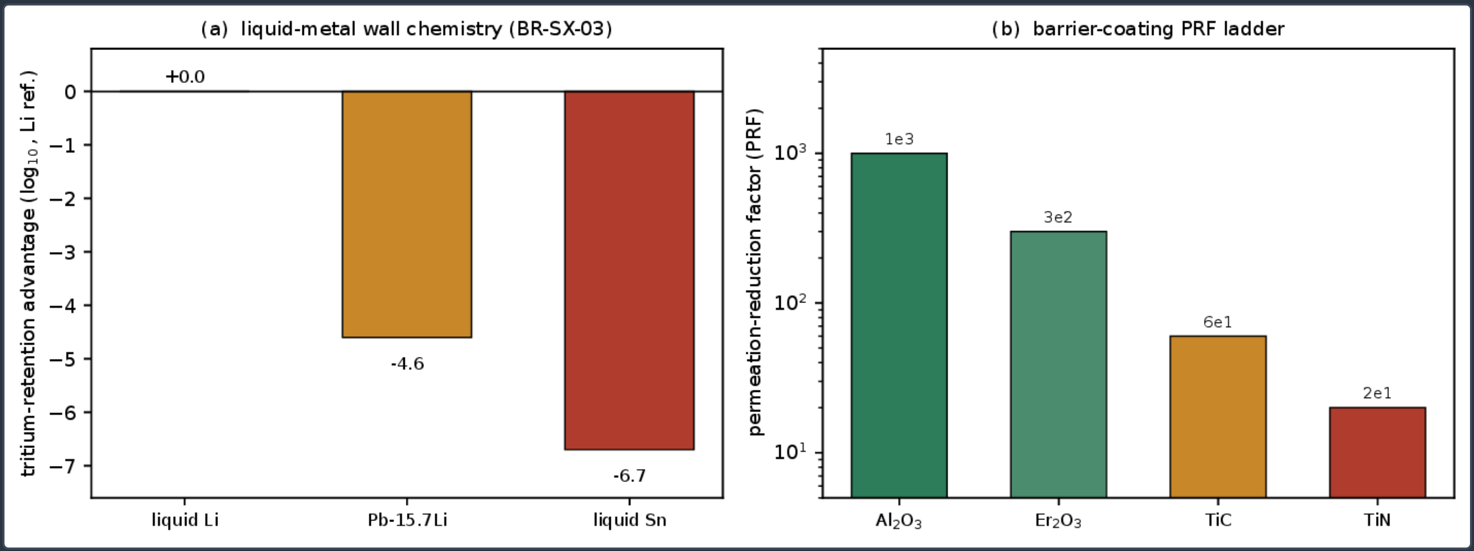

Tritium retention and permeation barriers (BR-SX-03). (a) Liquid-metal wall-chemistry retention advantage in orders of magnitude, lithium reference: Li $\gg$ Pb-15.7Li ($\mathbf{-4.6}$) $\gg$ Sn ($\mathbf{-6.7}$). (b) Permeation-reduction factor (PRF) ladder for candidate barrier coatings.

THE DOWN-SELECT

Figure 8 collapses the evaluation into the decision. The bare recipe is rejected on breeding; the beryllium-packed ceramic is the baseline (passes the bar with the frozen recipe, high maturity); the dedicated 5 cm solid-beryllium layer and the deeper blanket are the headroom and fine-adjust levers; and the self-cooled liquid-lithium blanket is retained as the thermally robust alternative with the strongest tritium-barrier margin of any candidate. Figure 9 shows the radial build that carries this selection—the shield-dominated inboard, the multiplier ahead of the outboard breeding zone, and the coverage geometry behind equation (13)—and figure 10 states the two-axis logic: a multiplier axis (none / packed / dedicated layer) and a breeder-form axis (ceramic / liquid Li).

Concept down-select scorecard for the Hyperion breeder blanket

	net TBR ≥ 1.05	thermal margin	tritium barrier	maturity	verdict
bare recipe (no multiplier)	0.742 fail	--	--	high	reject
Be-packed ceramic (reference)	1.03-1.06 pass	as-config. tight	adequate	high	BASELINE
ceramic + 5 cm solid-Be layer	1.18-1.20 pass	as-config. tight	adequate	med	headroom
deep blanket 65-80 cm	1.24-1.25 pass	as-config. tight	adequate	med	fine adjust
self-cooled liquid Li (alt.)	breeds + ^{7}Li($n,n'\alpha$)	516 °C +34	+6.7 orders vs Sn	med	RETAINED alt.

Concept down-select scorecard. Each concept is scored against the self-sufficiency bar, thermal margin, tritium barrier and maturity; the verdict column states the role each concept plays in the selection. Green = clears, amber = marginal/conditional, red = fails.

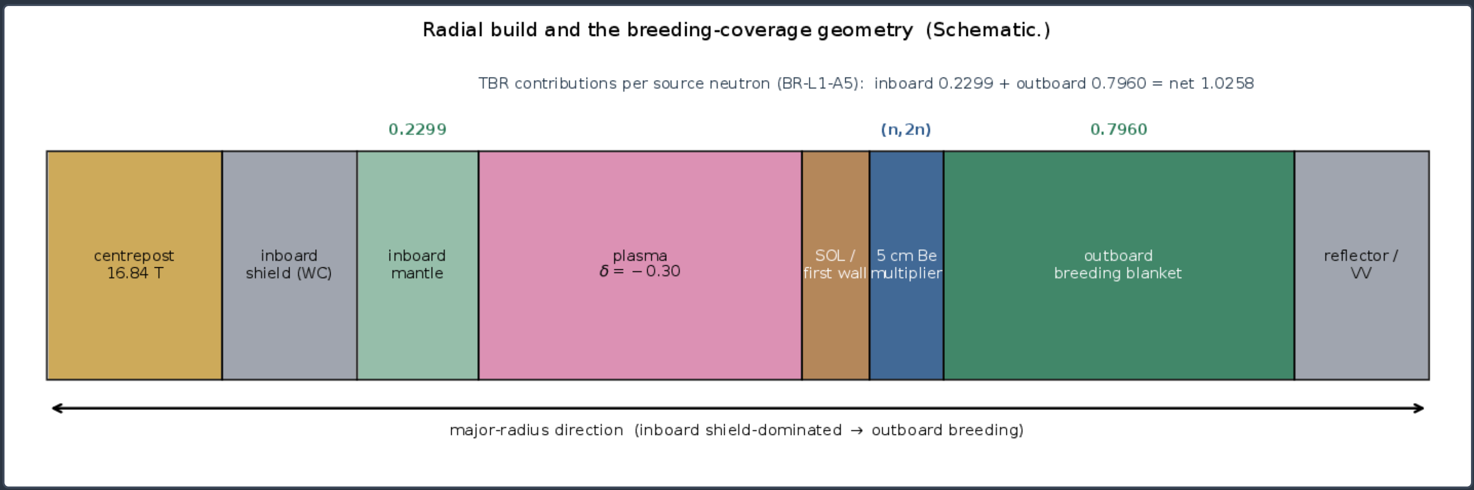

(Schematic.) Radial build and the breeding-coverage geometry. The centrepost (16.84 T) and its tungsten-carbide shield dominate the inboard; the outboard carries the dedicated 5 cm beryllium multiplier ahead of the breeding blanket. The TBR contributions per source neutron (inboard **0.2299** + outboard **0.7960**) are the additive ledger of equation (11). Layer widths are illustrative.

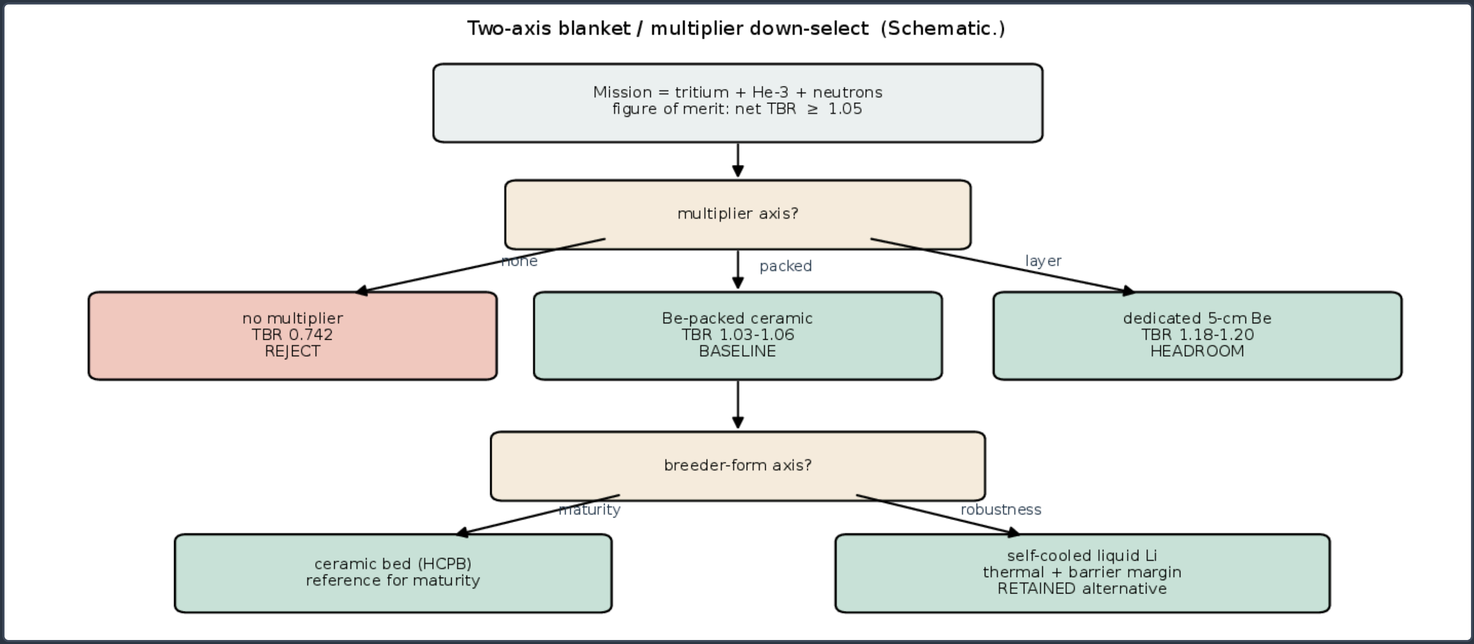

(Schematic.) The two-axis down-select. The multiplier axis carries the design from sub-unity (reject) through the beryllium-packed baseline to the dedicated-layer headroom; the breeder-form axis selects the ceramic bed for maturity and retains the self-cooled liquid-lithium blanket for thermal and fuel-cycle robustness.

§ 5

Discussion

AGAINST PUBLISHED BREEDING BENCHMARKS

The reference numbers sit squarely within the mainstream of blanket neutronics, which is the point: the Hyperion blanket is a conventional lithium/beryllium concept operated in an unconventional geometry. Published HCPB driver blankets for the EU DEMO report net TBRs in the 1.1–1.2 range with beryllium or beryllide multiplication [19,20], and the tritium self-sufficiency window analyses of Abdou and co-workers place the required net ratio near 1.05–1.15 once losses, decay and doubling are folded in [29,30]. Our resolved three-dimensional points (1.12 single null, 1.07 double null) and our reduced-order ladder (1.026–1.42) bracket that same window. Where the compact ST differs is not the chemistry but the coverage: equation (13) and figure 5 show that the binding constraint is the shield-dominated inboard, not the intrinsic breeding of lithium—which is why a design that would be comfortably self-sufficient at large aspect ratio must spend a multiplication or thickness lever to reach the same bar here. Table 3 places the concept against these benchmarks.

CONCEPT / STUDY	NET TBR WINDOW	MULTIPLIER
EU DEMO HCPB driver [19]	$\sim$ 1.1–1.2	Be / $Be_{12}Ti$ pebbles
EU DEMO WCLL / HCLL [22,21]	$\sim$ 1.1–1.2	Pb-15.7Li (self-multiplying)
self-sufficiency window [29,30]	$\gtrsim$ 1.05–1.15	(requirement, not a concept)
Kronos reduced-order ladder (this work)	1.026–1.42	packed Be $\rightarrow$ solid-Be stack
Kronos resolved 3-D CAD (this work)	1.07–1.12	solid-Be, coverage-honest

The Hyperion blanket concept against published breeding benchmarks. Values are net or near-net TBR windows; the Kronos entries are this work.

WHY THE LEVERS SEPARATE CLEANLY

The value of scoring the concepts on one ladder is that the derivation of §2 separates the levers. Multiplication (equation 10) is what carries the design from sub-unity to self-sufficient; blanket thickness (equation 12) is the fine, saturating adjustment; coverage (equation 13) is the compact-ST discount that the three-dimensional model resolves; and breeder form is a robustness and fuel-cycle choice (equations 15, 16–16) rather than a breeding one. Keeping both a ceramic and a liquid-lithium concept alive means the breeder is not hostage to a single blanket technology maturing on schedule, and the liquid-lithium option shares the flowing-lithium loop and its in-loop tritium recovery with the divertor down-select [9,10], so the second breeder form is not a standalone development but a system already carried elsewhere in the plant.

FLEET FRAMING

The single-unit result is a self-sufficiency machine, not a large exporter: the advanced solid-beryllium ceiling reaches $\Lambda = 1.42$, about 1.99 kg-T per unit per year (BR-L2-A7u), and the ST centrepost caps the inboard coverage that a higher ratio would require—Pb-15.7Li does not beat solid beryllium on this geometry across the tested configurations. The fleet path to a national tritium requirement is therefore a multi-unit argument, developed in the companion breeding-fleet and tritium-ladder papers [4,8], and it is the reason the mission is framed as self-sufficiency plus a modest surplus rather than single-unit export.

§ 6

Limitations

One honest gate bounds the selection. The dedicated multiplier layer and the deeper-blanket points buy net TBR with radial space (equation 2), which competes with the inboard centrepost shield; this radial-budget trade is the one open engineering item. It is bounded rather than open-ended, because self-sufficiency is already met at $\Lambda \geq 1.05$ in the resolved three-dimensional geometry (1.12 single null, 1.07 double null) *without* spending the full thickness lever—so the trade sets how much export headroom is affordable, not whether the breeder breeds. Two further caveats are stated plainly: the HCPB thermal verdict is an as-configured two-dimensional conjugate-heat-transfer result, not a full Navier–Stokes thermomechanical qualification, and the pass is contingent on the real vacuum-vessel heat path; and the liquid-lithium alternative inherits the magnetohydrodynamic pressure-drop and corrosion questions common to all flowing-lithium blankets, which the shared divertor loop [10] carries but this down-select does not close.

§ 7

Conclusion

Scored on a common three-dimensional continuous-energy Monte-Carlo footing against net TBR ≥ 1.05, the Hyperion breeder's blanket is a beryllium-multiplied ceramic bed: 0.742 bare, 1.026–1.062 with beryllium packing, and 1.18–1.20 with a dedicated 5 cm solid-beryllium layer, confirmed self-sufficient at 1.12 (single null) and 1.07 (double null) in real CAD geometry. The net ratio is an additive inboard-plus-outboard ledger ($0.2299 + 0.7960 = 1.0258$) whose three levers—multiplication, thickness, coverage—separate cleanly under the governing equations, and the surplus law $S = \dot{m}_{\rm burn}(\Lambda - 1)$ ties every ratio to a tritium product. A self-cooled liquid-lithium blanket is the thermally robust alternative—516 °C structure temperature against the 712 °C of an as-configured ceramic bed, and a ~ 6.7-order tritium-retention advantage over tin—and is retained as the second concept rather than discarded. The selection meets the breeder's tritium, helium-3 and neutron mission on both breeder forms; net electricity is explicitly not a criterion; and the multiplier thickness is the one lever that trades against the centrepost shield.

Acknowledgments tocsectionAcknowledgments Part of the Kronos Fusion Energy 2026 design series, a family-owned American company. The neutronics, activation and thermal-hydraulic computations ran on the Kronos NVIDIA GPU HPC campaign alongside an in-house HPC node for the reduced-order and analytic fuel-cycle layers. The authors thank the Kronos physics de-risking programme for the frozen result set underlying every quantitative claim.

Reproducibility. The blanket and multiplier results are register anchors—BR-L1-A5 (three-dimensional Monte-Carlo balance), BR-L1-A6 and BR-OUT-1 (fuel-cycle surplus law and startup inventory), BR-L2-A7 (beryllium multiplication lever), BR-L2-A11h and BR-L2-A7u (blanket-thickness and advanced-ceiling levers), HX-02 (coverage hardening), BR-SX-15 (blanket thermal-hydraulics) and BR-SX-03 (tritium-barrier chemistry)—in the Kronos Physics De-Risking Register (doi:10.5281/zenodo.22133057), and are regenerable from the archived OpenMC/DAGMC transport, CRAM-48 depletion, conjugate-heat-transfer and fuel-cycle decks. This paper is archived at its DOI doi:10.5281/zenodo.22645937; official version: https://www.kronosfusionenergy.com/publications/breeding-blanket-and-neutron-multiplier-concept-down-se.html and its official page https://www.kronosfusionenergy.com/publications/breeding-blanket-and-neutron-multiplier-concept-down-se.html.

Data availability tocsectionData availability This paper is archived at doi:10.5281/zenodo.22645937. The TBR-ladder inputs, the neutron-economy tallies, the fuel-cycle scripts and the thermal models used for the figures are archived with the deposit and reference the Kronos Physics De-Risking Register (doi:10.5281/zenodo.22133057). All quantitative values trace to the register by the serial identifiers cited inline. Any economic analysis is reported separately and is not part of the public deposit.

Competing interests tocsectionCompeting interests Provisional patent applications relating to aspects of this work have been filed.

tocsectionReferences

APPARATUS

Portfolio, People & Record

The intellectual-property estate, the people who built it, the limitations that gate it, and the sources it rests on.

1	4	40	27
GRANTED PATENT	2026 PROVISIONALS	TEAM MEMBERS	2022 PROVISIONALS

INTELLECTUAL PROPERTY

The patent portfolio

The estate spans a granted high-field magnet patent, pending utility and 2026 provisional filings that map to the two products, a digital-twin control provisional, a registered trademark application, and the original 2022 provisional family. Every patentable disclosure in the five-paper arXiv drop was protected **before** publication: the breeder and burner provisionals were filed 1–2 August, and a publication-gap omnibus filing the evening before the drop swept up the DEC, plasma-control, and REBCO-winding matter of the three otherwise-unprotected papers. Patent numbers and application serials are matters of public record; claim scope is summarised, not reproduced.

GRANTED & PENDING UTILITY

US 12,009,112	High-field tilted graded-REBCO magnet architecture (KRONO-002A) · *app. 17/878,550*	GRANTED
US 17/878,507	Core device / method (KRONO-001A) · *utility*	PENDING

2026 PROVISIONAL FILINGS — MAPPED TO THE PRODUCTS

64/124,209	Hyperion — spherical-tokamak tritium / helium-3 foundry · *breeder · filed Aug 2026*	FILED
64/124,220	Aegis / MetroVolt — synchrotron-cutoff, fuel-selection & plug-winding · *generator · filed Aug 2026*	FILED
64/115,167	KRONOS-CTRL digital-twin plant control · *provisional · filed Jul 2026*	FILED
64/005,440	Integrated spherical-tokamak fusion architecture · *early integrated-architecture filing · filed Mar 2026*	FILED
64/105,530	Negative-triangularity spherical-tokamak architecture · *foundational ST filing · filed Jul 2026*	FILED
64/128,097	Publication-gap omnibus — quasineutral two-species expander DEC · provenance-gated / latency-split plasma control · as-built high-field winding & conductor architecture · *filed 7 Aug 2026, the evening before the arXiv drop*	FILED

TRADEMARK & ORIGIN

FTK-98801894	Kronos Fusion Energy — trademark application	FILED
KR-2022-*	Original provisional family (KR-2022-00001 … 00027) · *27 filings, 2022*	PRIORITY

The narrow, defensible magnet novelty — the specific conductor and the digital-twin winding optimisation, not high-field REBCO as a category — is the commercial core that can earn ahead of any Q > 1 milestone, with markets in fusion magnet supply, MRI/NMR, accelerators, and proton therapy. The claim is scoped honestly: the high field is a *system field* result, not a stand-alone-coil record; the small-bore plug coil is structurally infeasible as a bare winding but resolved by a stress-managed structural shield (feasible-pending-FEA); and the winding-tape experiment returned a *null result*. The value is the method, not a field record.

THE TEAM

Founding partners, board, advisors & auditors

Kronos is built by a bench of advanced-fuel-fusion, high-field-magnet, direct-conversion, and materials specialists, with a board and operations team drawn from defense, national laboratories, and industry. Dates are shown as ranges; where a tenure has ended or is term-ending, the range says so.

FOUNDING PARTNERS — SCIENCE

Dr. Gerald Kulcinski
Co-Founder · Helium-3 & Advanced-Fuel Fusion
UW–Madison · 2023–Present

Dr. Carl Weggel
Chief Scientist / S.M.A.R.T. Design
MIT Alcator Program · 2022–Present

Dr. Robert J. Weggel
Magnetic Field Design
MIT Magnet Lab · 2022–Present

BOARD

Priyanca Ford
Founder & CEO · Executive Board
2022–Present

Bandel Carano
Finance / Strategy
Oak Investment Partners / Stanford · 2025–2026

Patrick Schweiger
Fusion Device Engineering
Oklo / CFS / TerraPower · 2025–Present

SCIENTIFIC ADVISORS

Dr. Steven O. Dean
Fusion Policy & History
DOE / Fusion Power Associates · 2025–Present

Dr. Patrick H. Diamond
Plasma Turbulence & Transport
UC San Diego · 2025–Present

Dr. Jack J. Dongarra
HPC & Numerical Algorithms
Turing Award · 2025–Present

Dr. Nasr M. Ghoniem
Chief Material Scientist
UCLA · 2025–Present

Dr. Siegfried Glenzer
Plasma Physics & Laser Fusion
Stanford / SLAC · 2022–Present

Dr. David A. Hammer
Pulsed-Power Fusion
Cornell · 2025–Present

Dr. Donald A. Spong
Plasma Theory & Confinement
ORNL · 2025–Present

Dr. Curtis Smith
Risk Assessment & Nuclear PRA
MIT / Idaho National Lab · 2025–Present

RADM (Ret.) David Goggins
Naval Engineering & Power-Plant Design
U.S. Navy · 2023–2026

Dr. Konstantin Batygin
Mathematician
Caltech · 2022–2025

Dr. Ruben Fair
Magnet Design / ITER Liaison
PPPL / Jefferson Lab · 2022–2025

Dr. Paul S. Weiss
Materials & Nanotechnology
UCLA · 2022–2025

SCIENTIFIC AUDITORS

Dr. Wilfred A. Cooper
Plasma Equilibrium Theory
EPFL / Swiss Plasma Center · 2025–Present

Dr. Ahmed Hassanein
Plasma–Material Interactions
Purdue / Argonne · 2025–Present

Dr. Patrick E. Hopkins
Extreme Thermal Materials
U. of Virginia · 2025–Present

Dr. Peter Hosemann
Materials Joining & Structural Integrity
UC Berkeley · 2025–Present

Dr. Travis W. Knight
Advanced Nuclear Fuels & Systems
U. of South Carolina · 2025–Present

Dr. Philippe Lebrun
Cryogenics & Magnet Cooling
CERN · 2025–Present

Dr. Nitendra Singh
Nuclear Safety & Fuel Cycle
ITER · 2025–Present

Dr. Guido Van Oost
Magnetic Confinement & Fusion Systems
Ghent University · 2025–Present

Dr. Gary S. Was
Radiation Materials & Structural Integrity
U. of Michigan · 2025–Present

Dr. Ray Sedwick
Direct Energy Conversion
U. of Maryland · 2025

OPERATIONS

Michael Laughlin
Chief Operating Officer
2022–Present

Martin Owens
Chief Strategy Officer
LANL / GE Hitachi · 2022–Present

MG (Ret.) Paul Pardew
Chief Contracting Officer
Army Contracting Command · 2022–Present

David Beck
Fusion Commercialization
U.S. Space Force · 2024–Present

Sushma Bhatia
Environmental & Legislative
Google · 2022–Present

Michael De Frenza
Technology Licensing
2023–Present

MG (Ret.) Robin L. Fontes
Cybersecurity & Defense
Army Cyber Command · 2022–Present

Vijay Gehani
Supply Chain & Components
INOX India · 2024–Present

Jon Michel Greenwood
IT & AI Infrastructure
Live Nation · 2023–Present

Brian C. O'Neill
National Security
CIA / ODNI · 2022–Present

Gen. (Ret.) Gustave F. Perna
DoD Liaison
Operation Warp Speed · 2022–2023

Andrea Romero
Marketing Lead
2022–Present

Legal counsel is retained; those roles are held on the internal roster and are not listed here.

SOURCES

References

1 P I Ford, *The Physics De-Risking Register: gate-by-gate evidence across a compact spherical-tokamak breeder and its D–^{3}He tandem-mirror burners*, Kronos Fusion Energy 2026 series. doi:10.5281/zenodo.22133057

2 P I Ford and G L Kulcinski, *Hyperion as a strategic-materials platform: gain, tritium breeding, He-3 co-production and 14 MeV neutron output from a compact spherical tokamak*, Kronos Fusion Energy 2026 series. doi:10.5281/zenodo.22645691. kronosfusionenergy.com/publications/breeder.html

3 P I Ford, *The Kronos strategic-materials platform: an integrated spherical-tokamak breeder and D–^{3}He tandem-mirror burner architecture with a helium-3 flywheel*, Kronos Fusion Energy 2026 series. doi:10.5281/zenodo.22645764. kronosfusionenergy.com/publications/integrated-platform-overview.html

4 P I Ford, *From tritium consumer to breeding fleet: net blanket TBR and the cross-library case for multi-unit tritium export from a compact spherical-tokamak breeder*, Kronos Fusion Energy 2026 series. doi:10.5281/zenodo.22645706. kronosfusionenergy.com/publications/blanket-tritium-breeding-lever.html

5 P I Ford, *CAD-faithful neutronics for a compact spherical-tokamak breeder: STEP-to-DAGMC Monte-Carlo transport reproducing the 3-D net tritium-breeding ratio*, Kronos Fusion Energy 2026 series. doi:10.5281/zenodo.22645881. kronosfusionenergy.com/publications/cad-faithful-neutronics-for-a-compact-spherical-tokamak.html

6 P I Ford, *Component activation, waste-class routing and decommissioning of a low-activation compact spherical-tokamak breeder*, Kronos Fusion Energy 2026 series. doi:10.5281/zenodo.22645846. kronosfusionenergy.com/publications/component-activation-waste-class-routing-and-decommissi.html

7 P I Ford, *Beryllium and $Be_{12}Ti$ neutron multipliers for a compact spherical-tokamak breeder: pebble performance, activation and closing net TBR ≥ 1.05*, Kronos Fusion Energy 2026 series. doi:10.5281/zenodo.22645889. kronosfusionenergy.com/publications/beryllium-and-be-ti-neutron-multipliers-for-a-compact-s.html

8 P I Ford and G L Kulcinski, *The tritium breeding ladder for a compact spherical-tokamak breeder: per-unit inventory, doubling time and the fleet path to tritium self-sufficiency*, Kronos Fusion Energy 2026 series. doi:10.5281/zenodo.22645746. kronosfusionenergy.com/publications/tritium-fuel-cycle-and-breeding-ladder.html

9 P I Ford, *A stacked detachment portfolio for a compact spherical-tokamak breeder: Super-X, double-null and snowflake geometries that cut the required argon seed fraction*, Kronos Fusion Energy 2026 series. doi:10.5281/zenodo.22645742. kronosfusionenergy.com/publications/divertor-portfolio.html

10 P I Ford, *A flowing-lithium vapor-box divertor with molten-salt in-loop tritium extraction for a compact spherical-tokamak breeder*, Kronos Fusion Energy 2026 series. doi:10.5281/zenodo.22645750. kronosfusionenergy.com/publications/flowing-lithium-vapor-box-divertor.html

11 P I Ford, *Blanket and divertor thermal-hydraulics for a compact spherical-tokamak breeder: coolant heat removal, peak-temperature margins and the walk-away safety case*, Kronos Fusion Energy 2026 series. doi:10.5281/zenodo.22645836. kronosfusionenergy.com/publications/blanket-and-divertor-thermal-hydraulics-for-a-compact-s.html

12 P I Ford, *Tritium permeation-barrier coatings for a compact spherical-tokamak breeder: the liquid-lithium-over-tin wall-chemistry choice*, Kronos Fusion Energy 2026 series. doi:10.5281/zenodo.22645870. kronosfusionenergy.com/publications/tritium-permeation-barrier-coatings-for-a-compact-spher.html

13 P K Romano and B Forget, The OpenMC Monte Carlo particle transport code, *Ann. Nucl. Energy* **51** 274 (2013).

14 P K Romano, N E Horelik, B R Herman, A G Nelson, B Forget and K Smith, OpenMC: a state-of-the-art Monte Carlo code for research and development, *Ann. Nucl. Energy* **82** 90 (2015). doi:10.1016/j.anucene.2014.07.048

15 D A Brown *et al*, ENDF/B-VIII.0: the 8th major release of the nuclear reaction data library, *Nucl. Data Sheets* **148** 1 (2018). doi:10.1016/j.nds.2018.02.001

16 P P H Wilson, T J Tautges, J A Kraftcheck, B M Smith and D L Henderson, Acceleration techniques for the direct use of CAD-based geometry in fusion neutronics analysis, *Fusion Eng. Des.* **85** 1759 (2010).

COLOPHON

How this document was made

The Kronos Fleet — Combined Editorial, 2026 is set in **Fraunces** (display), **Gelasio** (text), and **IBM Plex Mono** (data & equations), carried forward from the Kronos editorial design system.

The figures are rendered at 300 dpi from the deposited generator scripts; the document is composed as a single self-contained file with embedded fonts and imagery, paginated to US Letter, and rendered to PDF through a headless Chromium engine in matched light and dark editions.

Every headline quantity carries an evidence class; withdrawn and restated values are marked as such. Nothing herein is frozen beyond the founder-approved Tier-A set.

Explore it live — turn the interactive 3-D model, run the deposited solvers in the physics validator, and watch the companion film series.

LEGAL NOTICE

Notice, status, and distribution

Conceptual design & simulation study. This document reports a conceptual design and simulation study. It is not a construction commitment, a safety-analysis report, a regulatory filing, or an offer of securities. Forward-looking statements — schedules, costs, market sizes, and performance — are estimates subject to the limitations set out in the Simulations part and may change.

Numbers and their classes. Quantities are reported with evidence classes and case labels; modelled, assumed, and requirement-class values are identified as such and are not to be quoted without their labels.

Public edition. This edition carries the physics and design only; all financial, funding, and defense-commercial content has been removed for public distribution. The scientific text corresponds to the arXiv and journal submissions.

THE 2026 KRONOS SERIES

One programme, many papers

This editorial is one paper in the Kronos 2026 series — a real fusion company's complete, reproducible physics record for a spherical-tokamak breeder and its low-neutron D–^{3}He tandem-mirror burners. Every headline number is a frozen anchor in the Physics De-Risking Register.

Explore the whole programme: the De-Risking Register, the interactive 3-D model, and the physics validator.

KRONOS FUSION ENERGY

Breeding-Blanket and Neutron-Multiplier Concept Down-Select for a Compact Spherical-Tokamak Breeder: Ceramic versus Liquid-Metal Options Walking the TBR Ladder to Self-Sufficiency

A real fusion company building real machines. Explore the science, live.

Zenodo · doi:10.5281/zenodo.22645937

Read on kronosfusionenergy.com

The Physics De-Risking Register